Adsorption (2014) 20:701–711
DOI 10.1007/s10450-014-9614-z

Optimizing packing heterogeneity for sorption enhanced metathesis reaction

Saleh Rawadieh · Vincent G. Gomes · Ibrahem Altarawneh

Received: 4 April 2013 / Revised: 29 May 2014 / Accepted: 16 June 2014 / Published online: 25 June 2014

Abstract An equilibrium-limited heterogeneous catalytic reaction, propene metathesis is suitable for process intensification via sorption enhanced reaction. In this work, we investigate the effect of catalyst/adsorbent configuration for propene metathesis in conjunction with pressure swing reaction. The catalyst and adsorbent configuration variations were defined in terms of packing heterogeneity index (PHI) and their effects were investigated experimentally and theoretically. Model predictions were tested against experimental data with variable PHI and adsorption/reaction conditions, including the absence of heterogeneity and of separation process. The product 2-butene was strongly adsorbed and retained by the intermediate adsorbent layers, thereby increasing reactant concentration in the reaction zone and enhancing conversion and rate of reaction in the subsequent layer. Model predictions were found to agree reasonably with experimental data and were used to elucidate the mechanism and optimizing principle for such reactors.

Keywords Adsorption · Separation · Metathesis · Pressure swing reaction · Process intensification

S. Rawadieh · V. G. Gomes (✉) · I. Altarawneh
School of Chemical & Biomolecular Engineering, The University of Sydney, Sydney, NSW 2006, Australia
e-mail: v.gomes@usyd.edu.au

Present Address:
S. Rawadieh · I. Altarawneh
Department of Chemical Engineering, Al-Hussein Bin Talal University, Ma'an 71111, Jordan

List of Symbols

Variables

B	Langmuir adsorption coefficient (kg/mol)
C	Gas phase species concentration (mol/cm^3)
D_z	Axial dispersion coefficient (m^2/s)
K	Mass transfer coefficient (s^{-1})
L	Bed length (m)
$L_{C,k}$	Length of kth catalyst layer
$L_{A,k}$	Length of kth adsorbent layer
Nc	Number of components
P	Pressure (atm)
Pe	Peclet number
Q	Species concentration in adsorbed phase (mol/kg)
r_{rxn}	Rate of reaction (mol/s kg)
T	Temperature
t	Time (s)
u	Gas velocity (m/s)
$\bar{v}$	Dimensionless interstitial fluid velocity
x_{CA}	Catalyst/adsorbent volume ratio

Greek letter

x_i	Dimensionless solid-phase mole fraction
y	Gas phase mole fraction
z	Axial distance
α_i	Dimensionless mass transfer coefficient = k_iL/u
ε	Bed voidage
ϕ	Packing heterogeneity index
λ	Ethene production (mole/kg$_{cat/ads}$/s)
ρ	Density (kg/m^3)
υ_i	Stoichiometric coefficient of component *i*
τ	Dimensionless time
ξ	Mass capacity factor

Subscripts

Ads	Adsorbent
Cat	Catalyst
Feed	Feed stream
i	Gas species
P	Propene
B	Butene
E	Ethene
H	High pressure
L	Low pressure
S	Saturation

Superscripts

* Equilibrium condition

1 Introduction

Metathesis is a remarkable chemical reaction (Nobel Prize 2005; Chauvin 2006) in which the hydrocarbon molecules are fragmented at their double bonds to produce new molecules via recombination of fragments from the starting molecules. Olefin metathesis, in particular, is an industrially important reaction; for example, in propene metathesis, the generation of ethene and butene or vice versa is of significance in meeting shifting dynamic demands between poly(ethylene) or poly(propylene) (Herndon et al. 2007). The reaction has been exploited via the Phillips Triolefin Process (van de Graaf et al. 1999a, b) for commercial benefits. Thus, propene metathesis is useful for maximizing the production of ethene (forward reaction) or propene (reverse reaction) depending on demand:

$$2\ CH_2 = CHCH_3 \Leftrightarrow CH_2 = CH_2 + CH_3CH = CHCH_3$$

Propene metathesis, conducted with rhenium oxide on γ-alumina catalyst at room temperature, mainly yields primary metathesis products (Dragutan et al. 1985). In addition to industrial products from simple hydrocarbons, metathesis reactions are also of considerable interest in producing linear α-olefins, detergents, polymers, pheromones and perfume intermediates among others (Zhang et al. 2013; Grela 2010; Grubbs 2006; Schrock 2006).

Apart from increasing interests in the use of adsorbents for separation (García et al. 2013; Maring and Webley 2013), recent publications have highlighted the substantial benefits from process intensification through integrating reaction and separation processes (Jang et al. 2012; Chen et al. 2012). For equilibrium limited reactions, the advantages of coupling reaction with in situ separation in hybrid configurations has the potential to substantially improve conversion, product selectivity and establish favourable reaction equilibrium relative to conventional reactors (Sheikh et al. 2001; Xiu et al. 2002; Rawadieh and Gomes 2009; Beaver et al. 2010; van Selow et al. 2011). Further, such integrations are capable of significantly reducing equipment and plant costs.

Enhancements in propene conversion was reported with a silicalite-1 membrane reactor (van de Graaf et al. 1999a, b) and in a packed-bed reactor with zeolite adsorbent (Gomes and Yee 2002) using a pressure swing adsorption reactor (PSAR). The experiments were carried out using a packed bed in a dual-column unit under ambient temperatures. However, these studies provided no guidelines regarding the optimal arrangement of the catalyst and adsorbent and the effect of operating variables on the process and product.

Our aim here is to investigate variable catalyst/adsorbent layer configurations with propene metathesis to maximize the production of ethene as the prime product. Experimental and theoretical investigations with adsorptive reactors were conducted to elucidate the underpinning mechanism in determining the optimal configuration and operating conditions. Apart from the limiting configuration of fully homogeneous (or well-mixed) system, intermediate levels of heterogeneity in packing arrangement were investigated. For a packed bed reactor with multiple layers of catalyst and adsorbent, the PSAR system becomes a set of reactor-separators in series within the same vessel. The aim is to let 2-butene as a by-product be retained in the intermediate adsorbent layers temporarily to achieve increased propene conversion and enhanced reaction rate. The overall performance of the PSAR system is expected to depend on the arrangement.

2 Reactor-separator model

A dynamic model based on isothermal operation was developed to describe both the fixed-bed reactor (FBR) and sorption enhanced propene metathesis processes with variable catalyst/adsorbent configurations. An extended Langmuir model was used to describe adsorption equilibria, a linear driving force (LDF) model was used for mass transfer in adsorbent and the reaction kinetics was based on heterogeneous catalysis with product desorption as the rate limiting step. The principal model assumptions include axially dispersed plug flow system, ideal gas behavior, negligible radial dispersion, and packing with uniform particle size and bed voidage.

2.1 Model equations

The governing equations were converted into their dimensionless forms, where all dependent and independent variables were expressed in terms of dimensionless groups for a better representation of the parametric effects on the

process and to minimize the compounded truncation errors during the computation.

- Component mass balances in the catalyst/adsorbent phase are:

$$\frac{1}{P}\frac{\partial(P y_i)}{\partial \tau} = \frac{1}{Pe}\frac{\partial^2 y_i}{\partial z^2} - \frac{\partial(\bar{v} y_i)}{\partial \bar{z}} - \rho_{ads}\left(\frac{1-\varepsilon}{\varepsilon}\right)\left(\frac{q_{is}}{c_o}\right)\frac{\partial x_i}{\partial \tau} + \upsilon_i \bar{r}_{rxn}, \tag{1}$$

  where $c_o = \frac{P}{RT}$
- Overall mass balance in the catalyst/adsorbent phase are:

$$\frac{\partial \bar{v}}{\partial \bar{z}} = \frac{1}{P}\frac{\partial P}{\partial \tau} - \xi \sum_{i=1}^{Nc} \frac{q_{is}}{q_{is,ref}}\frac{\partial x_i}{\partial \tau} + \sum \upsilon_i \bar{r}_{rxn}, \tag{2}$$

  where $\xi = \rho_{ads}\left(\frac{1-\varepsilon}{\varepsilon}\right)\frac{q_{is,ref}}{c_o}$,where υ_i is the stoichiometric coefficient of species *i;* υ_i is negative for reactants and positive for products. Thus, $\upsilon_P = -2, \quad \upsilon_E = 1, \quad \upsilon_B = 1$ for propene (P), ethene (E) and 2-butene (B), respectively; z is dimensionless axial distance normalized with respect to total length L. The dimensionless rate of reaction is given by:

$$\bar{r}_{rxn} = \frac{r_{rxn}}{c_o}\frac{L}{u}\rho_{cat}$$

  The subscripts 'cat', 'ads' and 'ref' refer to the catalyst, adsorbent and reference species 2-butene, respectively.
- The reaction rate for propene metathesis (Gomes & Fuller 1996) is given by:

$$r_{rxn} = \frac{3.17 \times 10^{-4}\left(c_P^2 - \frac{c_B c_E}{0.0397}\right)}{c_P + 0.172c_P^2 + 2.309c_E + 2.727c_B + 0.398c_P c_E + 0.469c_P c_B} \tag{3}$$

- Component mass balance in the gas phase for 13× zeolite adsorbent layer:

$$\frac{1}{P}\frac{\partial(P y_i)}{\partial \tau} = \frac{1}{Pe}\frac{\partial^2 y_i}{\partial z^2} - \frac{\partial(\bar{v} y_i)}{\partial z} - \zeta_i \frac{\partial x_i}{\partial \tau}, \tag{4}$$

  where $\zeta_i = \rho_{ads}\left(\frac{1-\varepsilon}{\varepsilon}\right)\left(\frac{q_{is}}{c_o}\right)$
- Overall mass balance in the adsorbent layers:

$$\frac{\partial \bar{v}}{\partial z} = \frac{1}{P}\frac{\partial P}{\partial \tau} - \xi \sum_{i=1}^{Nc} \frac{q_{is}}{q_{is,ref}} - \frac{\partial x_i}{\partial \tau} \tag{5}$$

  Here, the subscript 'ads' refers to the adsorbent, zeolite 13×.
- The continuity equation to connect the PSAR steps is:

$$C_o = \sum_i \frac{P\, y_i}{RT} \neq f(z) \tag{6}$$

- Mass transfer rates: The LDF model is adopted to describe the mass-transfer rate of all components to the adsorbent, in dimensionless form

$$\frac{\partial x_i}{\partial t} = \alpha_i \left(x_i^* - x_i\right), \tag{7}$$

  where $\alpha_i = \frac{k_i L}{u}$
- Adsorption equilibrium:

$$x_i^* = \frac{b_i c_o y_i}{1 + \sum_i b_i c_o y_i} \tag{8}$$

2.2 Boundary and initial conditions

The boundary conditions for gas species at both ends (z = 0 and z = L) of the column are:

$$\frac{1}{Pe}\frac{\partial y_i}{\partial z}|_{z=0} = -\bar{v}|_{z=0}(y_{i,f} - y_i|_{z=0}); \quad \frac{\partial y_i}{\partial z}|_{z=L} = 0$$

The gas velocity boundary conditions are:

$$\bar{v}|_{z=0} = 1; \quad \frac{\partial \bar{v}}{\partial z}|_{z=L} = 0$$

and, the initial conditions of the process are:

$$y_i(z,0) = 0; \quad x_i = 0$$

The model equations were used for simulating the reactor/separator, solving them using the orthogonal collocation within the method of lines. Thirty collocation points are required in this case to obtain stable solutions with acceptable accuracy. At the collocation points, the overall mass balance equations were discretized to a set of algebraic equations which were solved by Gaussian elimination to obtain velocity distributions along the bed. Species material balances, discretized into a set of ordinary differential equations, were integrated in the time domain. Gear's stiff method was used for solving the resulting algebraic and ordinary differential equations to obtain the gas/solid phase concentration profiles along the reactor with time. Our model predictions were validated using experimental data obtained with multiple catalyst/adsorbent configurations.

3 Experimental setup

A stainless steel column of 10 mm diameter was packed with known amount of Re_2O_7 catalyst and zeolite 13× adsorbent. The flow rates of feed, product and purge streams were monitored by thermal mass flowmeters (Brooks, USA). Pressure gauges (PG) were used to monitor the column pressures. A micro-gas chromatograph (MTI, USA), equipped with a thermal conductivity detector (TCD) with two analysing channels was connected to the reactor/sorber to provide rapid ($\sim$20 s) on-line analysis of gas compositions. Typical process conditions used are noted below.

The catalyst, rhenium oxide (Re_2O_7) impregnated on gamma-alumina (γ-Al_2O_3) support, was prepared by incipient impregnation using ammonium perrhenate solutions. The catalyst was calcined by heating in air and activated by heating to 920 K in the presence of inert gas helium. The adsorbent zeolite 13× was used for the preferential sorption of 2-butene and propene at the reactor exit in order to obtain ethene as the desired value-added product at the outlet. The tests were carried out under ambient temperature conditions. Since the catalyst is highly selective, effects due to any side reaction were negligible.

4 Results and discussion

4.1 Reactor performance without adsorbent

The model was used to simulate propene metathesis for the following cases: reaction without adsorption (plug flow reactor, PFR), reaction with adsorption and reaction with PSAR. Adsorption equilibrium data of the adsorbates ethene, propene and 2-butene on γ-alumina and zeolite 13× were determined by adsorption chromatography and breakthrough tests by others (Gomes and Fuller 1994; Gomes and Yee 2002). The corresponding kinetic and equilibrium sorption parameters are given in Table 1. The isotherm parameters indicate that 2-butene has much greater sorption affinity among the three components involved. Thus the availability of sorbent surface for separation is expected to depend substantially on the removal efficiency of 2-butene from the reaction zone.

The catalyst was prepared in our laboratory and used after regenerating and testing for catalytic activity. The model was initially used to simulate a packed-bed reactor for an active catalyst with 5 mol % feed propene concentration. Experiments were conducted by passing a feed consisting of propene and nitrogen through the reaction/adsorption column at high pressure and flowrate. Nitrogen was used as an inert diluent to carry away the heat of reaction so that the isothermal conditions could be maintained. The product gas eluting from the column was continuously analysed by the MTI on-line gas chromatography until steady state conditions were attained.

Table 1 Kinetic and equilibrium data for ethene, propene, 2-butene

Entities	Units	Ethene	Propene	Butene
γ-Alumina				
$b_i \times q_{is}$	–	239.7	332.6	514.0
Saturation constant (q_{is})	mol kg^{-1}	0.1836	0.4106	0.8144
Zeolite 13×				
$b_i \times q_{is}$	–	29.5	12,690	58,780
Saturation constant (q_{is})	mol kg^{-1}	1.20	2.68	5.32
Diffusivity (D_e) × 10^5	$m^2\ s^{-1}$	3.29	2.05	1.47
LDF constant, k_i	s^{-1}	0.0325	0.0249	0.0211
$D_z \times 10^3$	$m^2\ s^{-1}$	1.30		

Figure 1 shows the species exit mole fractions as functions of dimensionless time, $\tau = tv_0/L$. The model predictions were found to be in reasonable agreement with the experimental data. The 2-butene produced comprises approximately equal proportions of the cis-2-butene and trans-2-butene isomers. A comparison between simulation and experimental results show that the model predicts slight differences in comparison to measured ethene, propene and 2-butene breakthrough times. The model predictions at steady state conditions are in reasonable agreement with experimental data, thereby suggesting that the catalyst was relatively stable during the experiment. We note that with fixed-bed operation, the bed reaches saturation and the exit concentrations of products ethene and 2-butene are only about 0.01 mol fraction. The experimental data are affected by measurement accuracy, time delay and gas dispersion effects which are approximately reflected in the models. The physical adsorption coefficients were obtained from pure species isotherms at small scale published elsewhere (Gomes and Fuller 1994) and are not available from theoretical considerations. In addition, the physical and chemical adsorptions interact that are only approximately accounted in the model. We note that the mild roll-up for ethene is not observed in the measured data at these low-level concentration measurements.

4.2 Variable reactor configurations with PSAR

Multilayer arrangements with k separated layers each comprising catalysts and adsorbents were considered. The layer configurations were organized such that the mass of catalyst and of adsorbent were kept constant throughout. Thus, the catalyst to adsorbent volume ratio, x_{CA}, was kept constant in each case:

$$x_{CA} = \frac{\sum_{i=1}^{k} L_{C,i} * (1 - \varepsilon_{C,i}) * A_{C,i}}{\sum_{i-1}^{k} L_{A,i} * (1 - \varepsilon_{A,i}) * A_{A,i}}, \quad (9)$$

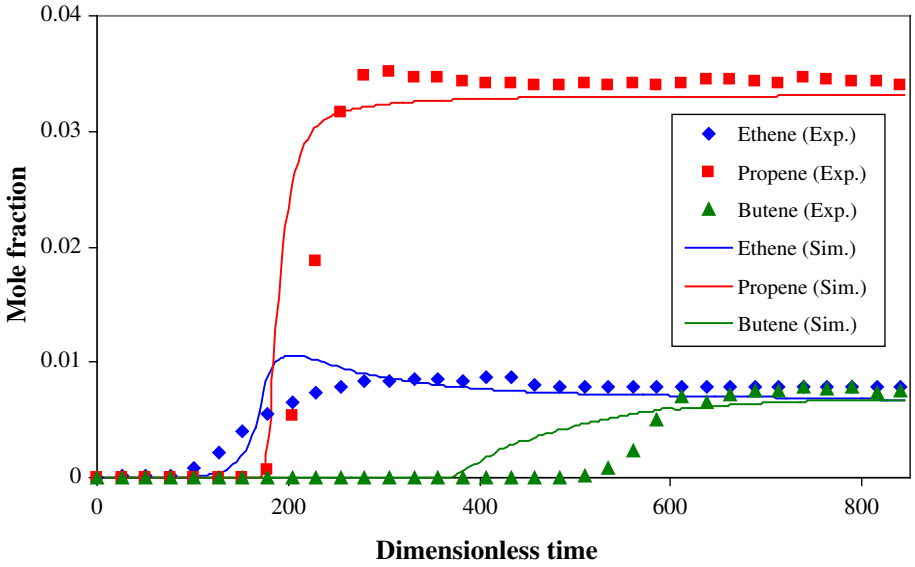

Fig. 1 Simulations and experimental data for exit mole fractions without adsorbent layer

where $L_{C,i}$ and $L_{A,i}$, are the lengths of the catalyst and adsorbent layer i, respectively. Since the cross-sectional area (A) and the void fraction (ε) is the same for both layers, the length of the layers determines the ratio. As the number of layers (k) increases, the catalyst-adsorbent bed approaches a homogeneously mixed configuration.

As an indication of the degree of heterogeneity of the catalyst/adsorbent mixture in the reactor, we defined a *packing heterogeneity index* (PHI or ϕ). PHI is equivalent to the inverse of number of layers, i.e., $\phi = 1/k$, where k is the number of catalyst or adsorbent layer. For example, if the bed is divided into two sections where the first section contains only the catalyst (layer one) and adsorbent in layer two, then the bed heterogeneity is maximum ($\phi = 1$). If two layers of catalyst and two layers of adsorbent are packed in alternating layers, then $\phi = 0.5$. For a well-mixed bed (i.e., for an infinite number of layers), the heterogeneity of the bed is at a minimum or $\phi = 1/\infty = 0$.

A value of $x_{CA} = 0.85$ was used to maintain equal mass deployment, i.e., the mass of catalyst equals that of the adsorbent. To reduce experimental error, the regenerated catalyst (Re_2O_7/γ-alumina) and adsorbent (zeolite 13×) were divided into separate portions for experiments with variable ϕ. Thus, identical columns were packed with equal amounts of catalyst and adsorbent, but with packing arrangements having ϕ ranging from 0 to 1. For $\phi = 1$ the column was divided into two sections separated by a porous filter paper. Catalyst particles were packed in the first section (near the feed end), while adsorbent particles were packed in the second section (near the exit). For $\phi = 0.5$, the column was packed sequentially with two layers each of catalyst and adsorbent and for $\phi = 0$, the column was packed with a uniform mixture of catalyst and adsorbent.

The performance of pressure swing process with variable ϕ was tested experimentally employing a twin-bed, four-step PSAR cycle:

- Pressurization (step 1): One column is pressurized to the operating pressure of the adsorption step with feed gas entering one end, while keeping the other end closed. During this stage, the species with the lower sorption affinity is forced towards closed end and enriched.
- Adsorption (step 2): The concentration wave-front developed at the pressurization step travels along the column such that the raffinate contains the less strongly adsorbed species. A portion of the raffinate is used as a feed to the second column for desorption, while the remainder is delivered as a product.
- Blowdown (step 3): The bed pressure is lowered, while counter-current flow reverses the direction of the travelling concentration wave-front of the less sorbed species. As a result, the product end of the bed is not contaminated with the more strongly adsorbed species.
- Counter-current purge (step 4): The raffinate from the adsorption step of bed 2 is used to desorb the adsorbates in bed 1, and to remove them from the voids so that their amounts are reduced at the start of the next cycle. Similar to blowdown, this step ensures that most of the strongly sorbed species is removed from the product end.

A step input in propene was introduced with nitrogen inert in feed, and the composition of the exit stream from the sorption/reaction step (step 1) was measured for all cycles until a cyclic steady state was attained.

Figure 2 shows experimental and simulation results for a two-bed PSAR with $\phi = 1$ under conditions given in

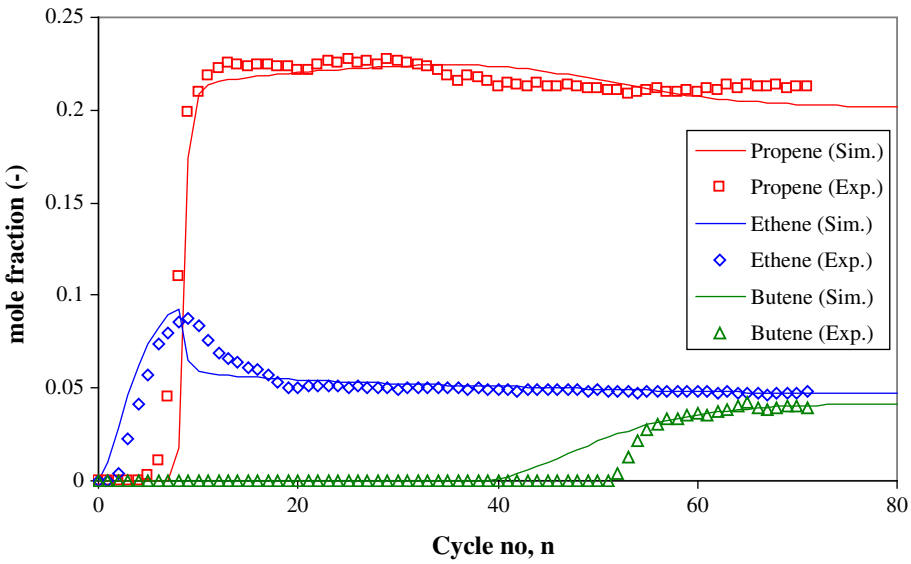

Fig. 2 Exit mole fractions at the end of adsorption/reaction step as a function of cycle number for $\phi = 1$ with regenerated catalyst and adsorbent

Table 2 Process operating conditions with variable packing heterogeneity index (ϕ)

Variables	$\phi = 1$	$\phi = 0.5$	$\phi = 0$
Column inside diameter (cm)	3.6	3.6	3.6
Catalyst bed length (cm)	8.05	8.05	–
Adsorbent bed length (cm)	9.45	9.45	–
Catalyst/adsorbent total length (cm)	17.5	17.5	17.5
Mass of catalyst (g)	58.23	58.21	58.25
Mass of adsorbent (g)	58.22	58.24	58.20
Catalyst/adsorbent mass ratio (g/g)	1:1	1:1	1:1
Feed pressure (atm)	3	3	3
Purge pressure (atm)	1	1	1
Purge to feed volume ratio	0.49	0.49	0.52
Adsorption/desorption time (s)	100	100	100
Blowdown/re-pressurization time (s)	20	20	20
Operating temperature (K)	291	291	291
Feed flowrate (at STP)			
Total	1,518	1,523	1,521
Nitrogen (mL min^{-1})	1,058	1,066	1,059
Propene (mL min^{-1})	460	457	462
Initial mole fraction (C/C_0)			
Propene	0.303	0.300	0.304
Nitrogen	0.697	0.700	0.696

Table 2. The products generated in the reaction zone and the unreacted reactants pass through the zeolite 13× layer, which selectively removes 2-butene and propene, leaving an ethene-rich product stream. We note reasonable agreement between model predictions and experimental data. Ethene has the lowest affinity to 13× zeolite and was the first component to exit from the product end, while butene has the highest affinity. Though the simulation indicates a somewhat earlier exit of ethene, the trend follows a pattern similar to those of experiments with reasonable prediction of steady state mole fraction of 0.05 and surge in ethene (0.09 mol frac) at the end of about 9th cycle (experimental data). The propene response simulation agrees with the experiments, except the time of propene appearance at the column exit.

Model predictions show a relatively gradual increase in 2-butene concentration profile compared to a slightly steeper response with lag for experiments. The slight mismatch in butene response indicates a possible variation in the empirical isotherm parameters adopted from the literature. Several factors including the non-uniformity in catalyst and adsorbent beds within the radial and axial domains affect the results. Nevertheless, the experimental and predicted trends are similar with reasonable agreement in steady-state values. Both experiments and simulations show that on using PSAR, and the consequent 2-butene removal from the reaction zone, ethene purity and yield are enhanced. The key issue with the gas mixture is that there are relatively strongly adsorbed species such as 2-butene and propene mixed with weakly adsorbed ethene. For pure gases, the adsorption isotherms were obtained under controlled conditions at small scale. Thereafter, the fitting with isotherm equations are not exact even with the extended Langmuir isotherm model. With mixtures of gases the behavior depends on the interactions between the competing molecules, the catalyst and sorbent, bed heterogeneity, flow nonuniformity and the unsteady-state nature of PSAR. The mixed gas behavior therefore is somewhat complex, especially when mixed gas behavior is derived from pure species isotherms using ideal solution theory. Thus perfect match between theory and experiment for a scaled up experimental facility is still quite difficult. For

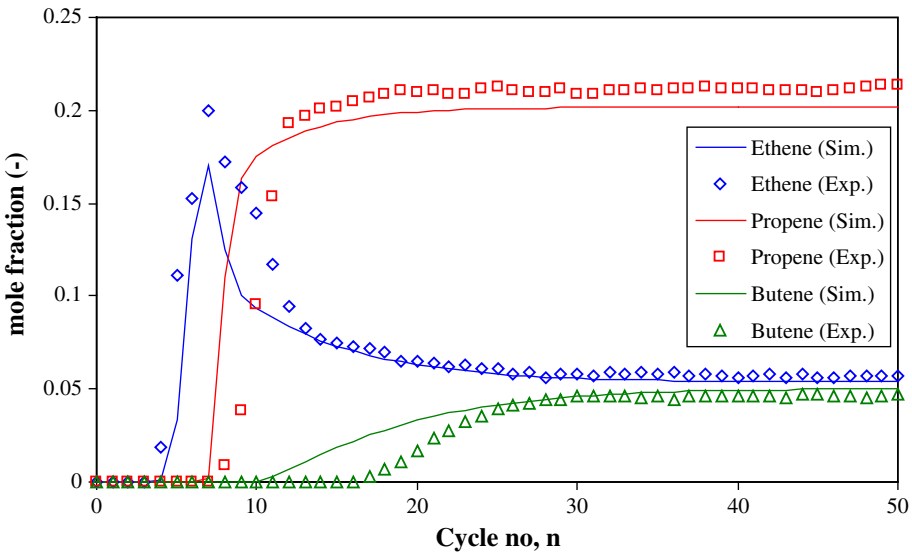

Fig. 3 Exit mole fractions at the end of adsorption/reaction step as a function of cycle number for $\phi = 0$ with regenerated catalyst and adsorbent

clarity, the authors have now mentioned the possible sources of errors for this process in the main text.

Intermediate layering ($0 < \phi < 1$) as well as well-mixed catalyst/adsorbent configurations ($\phi = 0$) were investigated via experiments and simulations. Results for the well-mixed configuration, Fig. 3 shows species composition as a function of cycle number. We note that the surge in ethene concentration is higher in this configuration than the previous one ($\phi = 1$). Ethene mole fraction is about 0.20 in the effluent stream at the seventh cycle and the ethene purity is enhanced in comparison. Further, 2-butene appears and reaches cyclic steady state (CSS) concentration much earlier.

In order to examine the effects of periodic separation internally due to PSAR with variable catalyst/adsorbent configuration, simulations were conducted for PSAR in a packed bed. The simulation results, showing changes in gas-phase mole fractions (y) as functions of bed length (z/L) and cycle number for propene metathesis PSAR with $\phi = 1$, are shown in Fig. 4. Ethene (Fig. 4a), due to its low sorption affinity is substantially affected by the sorption–desorption behavior of propene and 2-butene. Initially, the small amount of ethene formed is detected at the exit with no other component. Ethene concentration increases in the catalyst and decreases in the adsorbent zone; thus, it is detected after the first cycle for an initial its exit mole fraction of about 0.01. As the reaction proceeds, additional 2-butene and propene are preferentially adsorbed and ethene is largely displaced from the adsorbent between cycles one and eight.

The peak value in ethene concentration profile increases with the cycles as the concentration front progresses. Consequently, ethene exit concentration attains a maximum value of about 0.09 at cycle eight and thereafter equilibrates to a lower level of 0.05 at the exit. In contrast, propene shows moderate adsorption with no detection at bed exit until cycle eight. For a given cycle, propene mole fraction decreases along the bed and increases with cycle number before the CSS is attained. A final CSS is reached at a steady 0.21 mol fraction in about 40 cycles.

Figure 5 shows the gas-phase concentration profiles as functions of bed length (z/L) and cycle number for ethene and propene in a well-mixed PSAR configuration: $\phi = 0$. We note a lag in breakthrough of ethene in this case and ethene is first detected at bed exit after cycle four (compared to cycle one for $\phi = 1$). Thereafter, ethene reaches a peak mole fraction of about 0.17 at cycle seven. When the adsorbent is packed near the feed end, the adsorbent removes propene from the gas phase and reduces unadsorbed free propene in the bed, that is, the reactant is available to catalyst particles at a lower concentration. The interaction between reaction and separation increases when ϕ decreases, that is when 13× zeolite and catalyst solids mixture approaches the well-mixed configuration ($\phi = 0$). Figure 5a shows that the peak value of ethene concentration in PSAR with $\phi = 0$ is the highest (0.17 mol/mol) compared to other configurations.

The mole fraction of propene at feed end ($z/L = 0$) increases with cycle number. However, the mole fractions of propene at the feed end of the bed between different cycles are more dispersive for a low heterogeneity index: $\phi = 0$ (Fig. 5b), relative to a bed with high heterogeneity index (Fig. 4b). Figure 5b shows that propene elutes at cycle seven (a cycle earlier compared to the discrete layer configuration). However, the exit mole fraction of propene for $\phi = 1$ is greater than that in bed configuration with $\phi = 0.5$ but is much lower than that in a well mixed configuration ($\phi = 0$). This is due to the complex

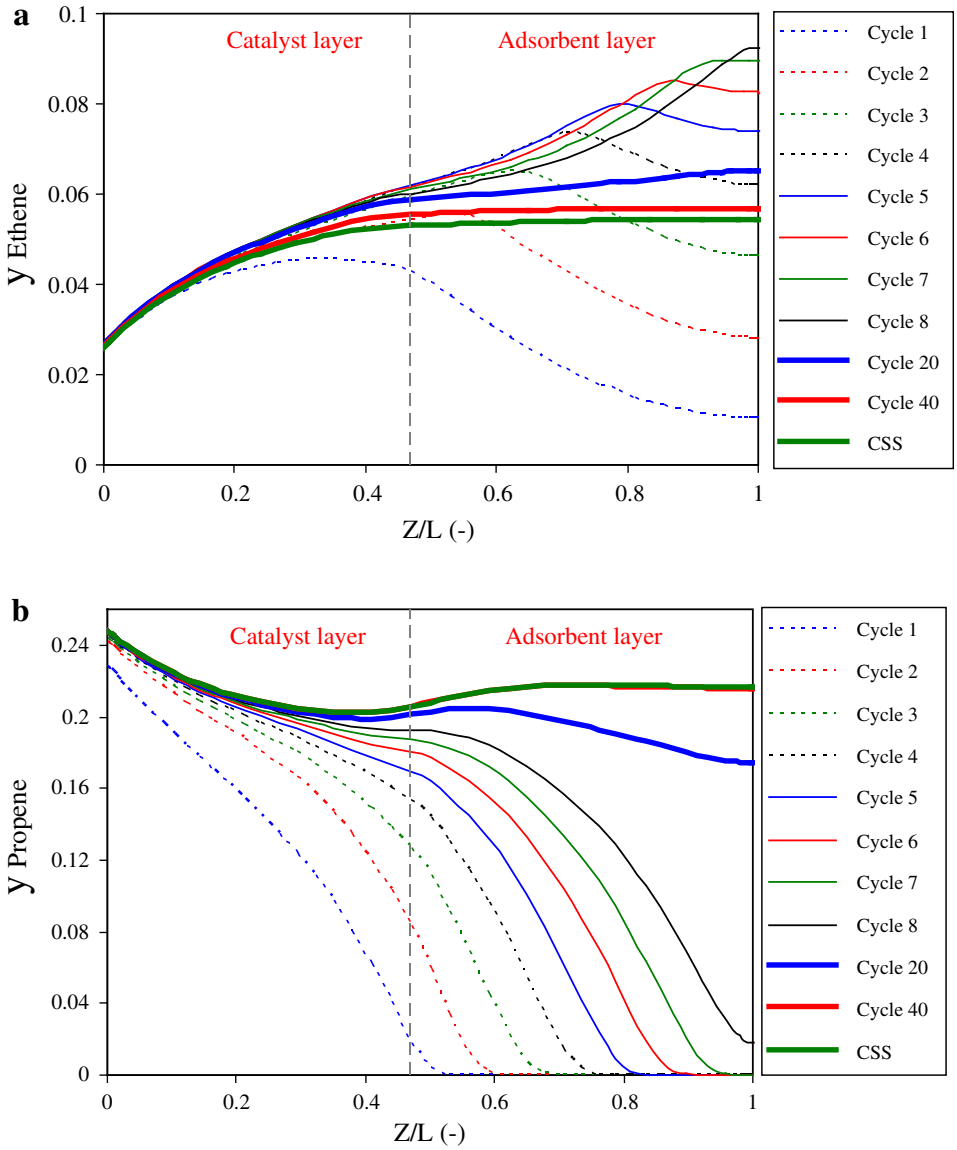

Fig. 4 Gas-phase concentration profiles as functions of column length (z/L) and cycle number (n) at the end of adsorption/reaction step for $\phi = 1$. **a** Ethene mole fraction, **b** propene mole fraction

interaction of adsorption of reactant and enhancement of conversion with decrease in heterogeneity of PSAR beds.

4.3 PSAR performance as a function of ϕ

Analysis of PSAR performance as a function of PHI (Table 3) shows that the steady state concentration of ethene and butene are almost equal for a fixed bed reactor with and without adsorbent, that is, the selectivity of ethene is about 1. For a multilayer configuration and no PSAR effect, the lack of catalyst and adsorbent regeneration leads to less than optimal reactor performance. Table 3 shows that the use of PSAR for the same configuration has several advantages. First, higher purity of ethene is obtained with PSAR; with $\phi = 1$, ethene constitutes about 17.3 % of the product, while only 11.0 % ethene purity is obtained without the pressure swing effect. Further, with pressure swing reaction, the selectivity for ethene over 2-butene is increased by 67 % for PSAR ($\phi = 1$) relative to without PSAR. We note that the productivity of catalyst and adsorbent, ethene recovery, yield and conversion increase significantly when PSAR is applied.

Table 3 shows that the reactor performance is enhanced with decrease in ϕ, i.e., with reduction in packing heterogeneity of catalyst and adsorbent. Thus, a well-mixed configuration ($\phi = 0$) provides improved propene conversion, yield, ethene recovery, ethene purity and solid productivity. However, ethene selectivity is optimal for bed configuration with $\phi = 0.5$. This is because of the relative sorption affinities for the three species. Though reduced bed heterogeneity maximizes overall gains in reactor performance, from a practical point of view a homogeneous catalyst/adsorbent mixture has certain disadvantages, such

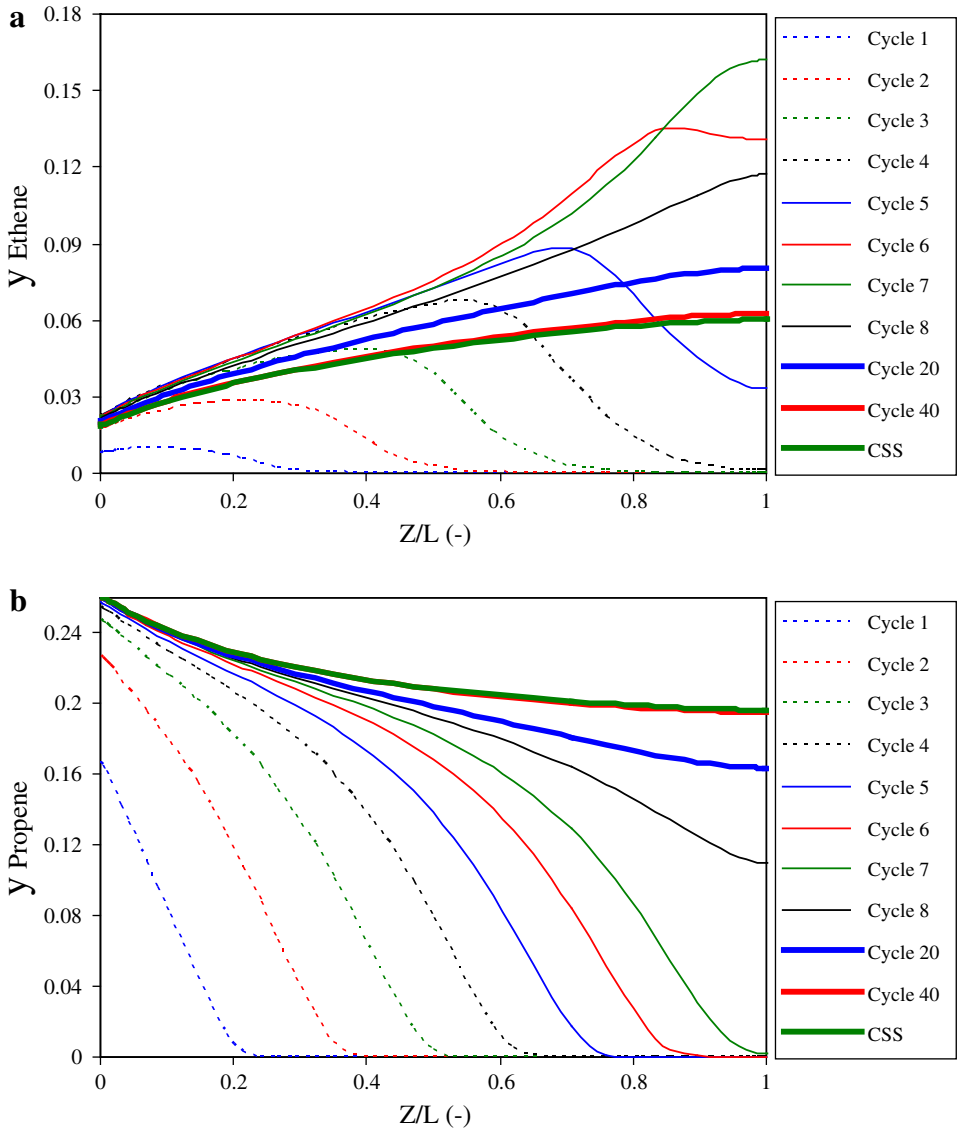

Fig. 5 Gas-phase concentration profiles as functions of column length (z/L) and cycle number (n) at the end of adsorption/reaction step for $\phi = 0$. **a** Ethene, **b** propene

Table 3 Effect of catalyst and adsorbent configuration on PSAR performance

Performance parameters	Reactor operation without PSAR	$\phi = 1$	$\phi = 0.5$	$\phi = 0.25$	$\phi = 0$
Purity (%)	11.0	17.3	18.0	18.4	19.3
Recovery (%)	–	77.5	80.4	82.9	88.3
Selectivity	1	1.67	1.97	1.88	1.81
Yield (%)	21.2	28.4	30.2	31.0	34.7
Conversion (%)	26.1	30.3	31.9	33.4	35.6
Productivity (mol $kg^{-1}s^{-1}$) $\times 10^4$	3.32	5.81	6.13	6.22	6.86

as, difficulties with separating a solid mixture, subjecting differential treatment or regeneration process and replacement of either the catalyst or the adsorbent individually.

4.4 Effect of cycle time

With PSAR, the interactions between the reaction and sorption/desorption steps are subtle and depend on the cycle and step times of the process. The cyclic step durations are often selected based on: (a) equal adsorption/desorption times; (b) adsorption termination before breakthrough; and (c) consideration of reaction rate and catalyst deactivation. In a majority of the cases, the service time of catalyst between two consecutive regenerations is far longer than the breakthrough time of catalyst/adsorbent bed; thus, the breakthrough time is often the key criteria.

The process cycle time effect on propene metathesis was investigated for heterogeneous ($\phi = 1$) and homogeneous bed configurations ($\phi = 0$). Both pressurization and blowdown times were kept the same (20 s for each) and the catalyst was regenerated before loading into the column.

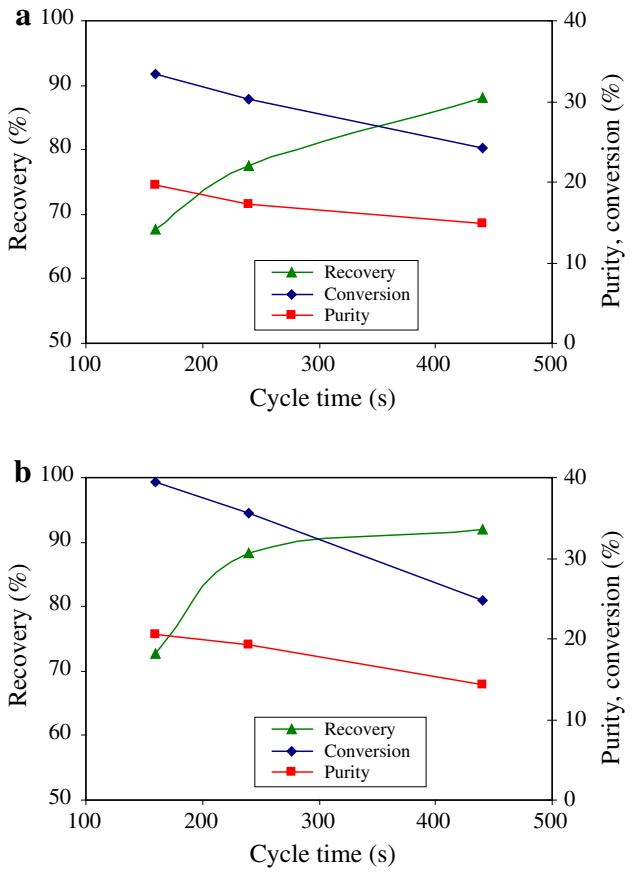

Fig. 6 Effect of cycle time on propene metathesis PSAR performance, recovery, purity of ethene and conversion of propene. **a** $\phi = 1$, **b** $\phi = 0$

The cycle time was varied between 160 and 440 s, where equal adsorption and desorption step cycle times were allocated in each case. The results obtained from our simulations are shown in Fig. 6. The simulations are in agreement with experimental data except for early 2-butene elution for simulations. Increasing the frequency of adsorbent regeneration is expected to improve separation to a certain extent with enhanced conversion due to improved intensification for well-mixed configuration (PHI = 0).

For both catalyst/adsorbent packing arrangements, simulations show that PSAR with a relatively short cycle time is favoured as higher propene conversion and ethene purity is obtained, because of the increase in the adsorbent regeneration frequency. This is demonstrated in Fig. 6a, b where propene conversion increases significantly with a slight increase in ethene purity when total cycle time is decreased from 440 to 160 s. However, this occurs at the expense of ethene recovery which is reduced from more than 90–70 %.

Figure 6b shows that the recovery of ethene for PSAR with $\phi = 1$ at cycle time of 160 s is higher than that for $\phi = 0$. As indicated earlier, the separation of 2-butene from the product stream becomes less efficient with a lower cycle time of 160 s, as the purity decreases. For $\phi = 1$, the purity and recovery curves intersect at about 200 s. In contrast, for $\phi = 0$, the purity and recovery curves intersect at 160 s to provide improved ethene purity, ethene recovery and propene conversion. The simulations are consistent with the trends shown by experiments, indicating that a well-mixed configuration with a relatively lower cycle time provides an improved reaction/separation performance.

5 Conclusion

The effect of catalyst/adsorbent configuration was determined for propene metathesis in conjunction with pressure swing reaction. Packing configurations were defined in terms of packing heterogeneity index (PHI, ϕ) and their effects were investigated experimentally as well as theoretically. Model predictions were tested against experimental data with variable adsorptive reactor configurations. Simulations were in reasonable agreement with experimental data. For a sequentially packed bed with several layers of catalyst and adsorbent, the adsorption/reaction bed behaved as a set of reactor/separators in series. The product 2-butene was strongly adsorbed and retained by the intermediate adsorbent layers, thereby increasing the reactant concentration in the reaction zone and enhancing propene conversion and the rate of reaction in the subsequent layer. The well-mixed reactor configuration was found to have a number of advantages relative to discrete layers in terms of overall conversion, product purity, product recovery and yield. However, the selectivity diminishes slightly relative to intermediate layering with $\phi = 0.5$. PSAR with a relatively short cycle time provides higher propene conversion and higher ethene purity due to the increased frequency of adsorbent regeneration.

Acknowledgments The authors acknowledge the award of a postgraduate studentship by Al-Hussein Bin Talal University (Jordan) and support from the Australian Research Council (ARC).

References

Beaver, M.G., Caram, H.S., Sircar, S.: Sorption enhanced reaction process for direct production of fuel-cell grade hydrogen by low temperature catalytic steam–methane reforming. J. Power Sources **195**, 1998–2002 (2010)

Chauvin, Y.: Olefin metathesis. Angew. Chem. Int. Ed. **45**, 3740–3747 (2006)

Chen, S., Xiang, W., Wang, D., Xue, Z.: Incorporating IGCC and CaO sorption-enhanced process for power generation with CO_2 capture. Appl. Energy **95**, 285–294 (2012)

Dragutan, V., Balaban, A.T., Dimonie, M.: Olefin Metathesis and Ring-Opening Polymerization of Cycloolefins. Wiley, New York (1985)

García, S., Gil, M.V., Pis, J.J., Rubiera, F., Pevida, C.: Cyclic operation of a fixed-bed pressure and temperature swing process for CO_2 capture: experimental and statistical analysis. Int. J. Greenh. Gas Control **12**, 35–43 (2013)

Gomes, V.G., Fuller, O.M.: Fixed-bed adsorber dynamics in binary physisorption-diffusion. Can. J. Chem. Eng. **72**, 622–630 (1994)

Gomes, V.G., Fuller, O.M.: Dynamics of propene metathesis: physisorption and diffusion in heterogeneous catalysis. AIChE J. **72**, 622–630 (1996)

Gomes, V.G., Yee, K.W.K.: A periodic separating reactor for propene metathesis. Chem. Eng. Sci. **57**, 3839–3850 (2002)

Grela, K.: Progress in metathesis chemistry. Beilstein J. Org. Chem. **6**, 1089–1090 (2010)

Grubbs, R.H.: Olefin-metathesis catalysts for the preparation of molecules and materials. Angew. Chem. Int. Ed. **45**, 3760–3765 (2006)

Herndon, J.W., Robert, H.C., Mingos, D.M.P.: Metathesis Reactions. Comprehensive Organometallic Chemistry III. Elsevier, Oxford (2007)

Jang, H.M., Lee, K.B., Caram, H.S., Sircar, S.: High-purity hydrogen production through sorption enhanced water gas shift reaction using K_2CO_3-promoted hydrotalcite. Chem. Eng. Sci. **73**, 431–438 (2012)

Maring, B.J., Webley, P.A.: A new simplified pressure/vacuum swing adsorption model for rapid adsorbent screening for CO2 capture applications. Int. J. Greenh. Gas Control **15**, 16–31 (2013)

Nobel Prize in chemistry: development of the metathesis method in organic synthesis. http://www.nobelprize.org/nobel_prizes/chemistry/laureates/2005/ (2005). Accessed 10 Mar 2013

Rawadieh, S., Gomes, V.G.: Steam reforming for hydrogen generation with in situ adsorptive separation. Int. J. Hydrogen Energy **34**, 343–355 (2009)

Schrock, R.R.: Multiple metal–carbon bonds for catalytic metathesis reactions. Angew. Chem. Int. Ed. **45**, 3748–3759 (2006)

Sheikh, J., Kershenbaum, L.S., Alpay, E.: 1-butene dehydrogenation in rapid pressure swing reaction processes. Chem. Eng. Sci. **56**, 1511–1516 (2001)

van De Graaf, J.M., Zwiep, M., Kapteijn, F., Moulijn, J.A.: Application of a silicalite-1 membrane reactor in metathesis reactions. Appl. Catal. A **178**(2), 225–241 (1999a)

van De Graaf, J.M., Zwiep, M., Kapteijn, F., Moulijn, J.A.: Application of a zeolite membrane reactor in the metathesis of propene. Chem. Eng. Sci. **54**, 1441–1445 (1999b)

van Selow, E.R., Cobden, P.D., Wright, A.D., van den Brink, R.W., Jansen, D.: Improved sorbent for the sorption-enhanced water-gas shift process. Energy Procedia **4**, 1090–1095 (2011)

Xiu, G., Li, P., E. Rodrigues, A.: Sorption-enhanced reaction process with reactive regeneration. Chem. Eng. Sci. **57**, 3893–3908 (2002)

Zhang, H., Li, Y., Shao, S., Wu, H., Wu, P.: Grubbs-type catalysts immobilized on SBA-15: a novel heterogeneous catalyst for olefin metathesis. J. Mol. Catal. A **372**, 35–43 (2013)